Effect of Initial Moisture Content and Type of Surface Finish Layers on the Energy Performance of a Residential House with Cellular Concrete Walls

Dariusz J. Gawin, D.Sc. **Jan Kosny, Ph.D.**

ABSTRACT

The hygrothermal behavior of an external, 8 in. cellular concrete wall was numerically simulated for the first three years of building use. A state-of-the art model of coupled heat, air, and moisture transfer in deforming porous building materials, HMTRA-DEF, was used for the simulation. Climatic data for a typical meteorological year for Sacramento, California, and Miami, Florida, were applied for the definition of external boundary conditions. Four different cases for finish layers—interior and exterior wall surfaces, with and without a vapor-retardant paint—were considered. Based on the simulation results, space- and time- averaged values of moisture content, thermal conductivity, apparent density, and specific heat of the cellular concrete layer were calculated for each month. These averaged material properties were used for a DOE-2.1E simulation of the whole-building energy performance of a 143.1 m^2 (1540 ft^2) residential house for each month of the analyzed period. Additionally, monthly values were calculated for energy released or absorbed on the internal surface of the wall as a result of the condensation or evaporation process. These results have been used to approximate, for various types of finish layers on the external walls, the effect of technological moisture drying on the energy performance of the whole building during the first few years of its use. The results of the analysis are presented and discussed.

INTRODUCTION

Cellular concrete is a building material whose thermal properties, especially thermal conductivity, strongly depend on moisture content (Gawin et al. 2000). This feature is of importance mainly during the first period of use of a building with cellular concrete walls, when they still contain large amounts of water from construction. This water evaporates later. In spite of the fact that moisture content is a significant factor affecting the thermal conductivity of cellular concrete, the thermal properties of dried materials are commonly used for simulations of whole-building energy performance.

There are no reliable hygrothermal computer models of the whole building that take into account all physical phenomena important both to the behavior of individual building elements and to whole-building energy performance. While some models have attempted to meet this need (Kohonen 1984; Burch et al. 1990; Pedersen 1990; FSEC 1992), these computer programs are based on simplified models of either nonisothermal moisture transport (FSEC 1992) or whole-building mass and energy exchange (Kariagiozis et al. 1994). In this paper, an approximate method has been applied. The hygrothermal behavior of cellular concrete wall has been simulated by a coupled heat, air, and moisture transfer computer model.

Currently, several hygrothermal models are available—for example, TRATMO (Kohonen 1984; Salonvaara and Karagiozis 1994), MOIST (Burch et al. 1990; Burch et al. 1996), MATCH (Pedersen 1990; Rode and Courville 1991), WUFI (Kuenzel 1994), Latenite (Kariagiozis et al. 1994), and HMTRA (Gawin et al. 1995, 1996; Gawin and Schrefler 1996). HMTRA was chosen for the analysis presented in the following section of this paper. After some modifications, the HMTRA computer code allowed us to calculate the latent heat absorbed and released on the internal surface of the wall during the moisture drying/vapor condensation processes.

Dariusz Gawin is an associate professor in the Department of Building Physics and Building Materials, Technical University of Lodz, Lodz, Poland. **Jan Kosny** is a staff scientist at Oak Ridge National Laboratory, Oak Ridge, Tenn.

MATHEMATICAL MODEL OF COUPLED MASS AND ENERGY TRANSFER IN BUILDING MATERIALS

The mathematical model used in this paper to describe the hygrothermal behavior of deformable building materials was originally derived by Gawin, Baggio, and Schrefler (1995). The following paragraphs briefly summarize some of the main features of the model and information about its numerical solution.

The model treats building materials as multiphase media, where solid skeleton voids are filled partly with liquid water (capillary and adsorbed water) and partly with gas-phase water (an ideal mixture of dry air and water vapor). The full model consists of balance equations for the following:

- the mass of the solid skeleton;
- the mass of dry air, considering both diffusional (Fickian) flow and advectional (Darcian) flow molecule transport mechanisms;
- the mass of the water species, in both liquid and gaseous state, taking into account phase changes (i.e., evaporation–condensation, adsorption–desorption, hydration–dehydration) and diffusional and advectional transport mechanisms for gas molecules;
- the enthalpy of the whole medium, with the latent heat of phase changes and the heat effects of the hydration-dehydration processes, along with consideration of energy transport by both conduction and convection; and
- the linear momentum (mechanical equilibrium) of the multiphase system, taking into account elastic deformation and thermal expansion.

These equations are completed by an appropriate set of constitutive and state equations, initial and boundary conditions, and some thermodynamic relationships. Temperature, capillary pressure, and the gas-pressure dependence of several material parameters (e.g., sorption isotherms, thermal conductivity and capacity, intrinsic and relative permeability, effective vapor diffusivity, Young's modulus, and Poisson's ratio) are taken into account. The main physical quantities (e.g., specific latent heat of evaporation and adsorption, water and gas viscosity, and vapor diffusivity in the air) are also taken into account.

The governing equations of the model are expressed in terms of the chosen state variables—that is, gas pressure, $\boldsymbol{p_g}$; capillary pressure, $\boldsymbol{p_c}$; temperature, $\boldsymbol{T}$; and displacement vector of the solid matrix, $\boldsymbol{u}$.

After application of the finite element method (Galerkin's type, weighted residuals procedure) (Zienkiewicz and Taylor 1989, 1991) for space discretization, these equations may be written in compact matrix form as

$$\boldsymbol{C}(\boldsymbol{x})\dot{\boldsymbol{x}} + \boldsymbol{K}(\boldsymbol{x})\boldsymbol{x} + \boldsymbol{f}(\boldsymbol{x}) = 0 \tag{1}$$

where $\boldsymbol{x} = \left\{\overline{\boldsymbol{p_g}}, \overline{\boldsymbol{p_c}}, \overline{\boldsymbol{T}}, \overline{\boldsymbol{u}}\right\}^T$ is a vector of unknown state variables, and the elements of the nonlinear matrix coefficients $\boldsymbol{C}(\boldsymbol{x})$, $\boldsymbol{K}(\boldsymbol{x})$, and $\boldsymbol{f}(\boldsymbol{x})$ are specified in detail in Gawin et al. (1996).

The time discretization is accomplished by means of a fully implicit finite difference scheme (backward difference) (Zienkiewicz and Taylor 1989, 1991):

$$\boldsymbol{C}_{n+1}\frac{\boldsymbol{x}_{n+1}-\boldsymbol{x}_n}{\Delta t} + \boldsymbol{K}_{n+1}\boldsymbol{x}_{n+1} + \boldsymbol{f}_{n+1} = 0 \tag{2}$$

where $\boldsymbol{C}_{n+1}= \boldsymbol{C}(\boldsymbol{x}_{n+1})$, $\boldsymbol{K}_{n+1}= \boldsymbol{K}(\boldsymbol{x}_{n+1})$, $\boldsymbol{f}_{n+1}= \boldsymbol{f}(\boldsymbol{x}_{n+1})$, n is the time step number, and Δt is the length of the time step.

Because of the nonlinearity of Equation 2, the solution is obtained with a Newton-Raphson type procedure (Zienkiewicz and Taylor 1989, 1991):

$$\begin{aligned}
&\frac{1}{\Delta t}\left[\frac{\partial \boldsymbol{C}^1_{n+1}}{\partial \boldsymbol{x}}(\boldsymbol{x}^1_{n+1}-\boldsymbol{x}_n) + \boldsymbol{C}^1_{n+1}\right]\Delta\boldsymbol{x}^1_{n+1} \\
&+\left[\frac{\partial \boldsymbol{K}^1_{n+1}}{\partial \boldsymbol{x}}\boldsymbol{x}^1_{n+1} + \boldsymbol{K}\boldsymbol{x}^1_{n+1} + \frac{\partial \boldsymbol{f}^1_{n+1}}{\partial \boldsymbol{x}}\right]\Delta\boldsymbol{x}^1_{n+1} \\
&= -\left[\boldsymbol{C}^1_{n+1}\frac{\boldsymbol{x}^1_{n+1}-\boldsymbol{x}_n}{\Delta t} + \boldsymbol{K}^1_{n+1}\boldsymbol{x}_{n+1} + \boldsymbol{f}^1_{n+1}\right]
\end{aligned} \tag{3}$$

where l is the iteration index, and at the end of each iteration, the primary variables are updated as follows:

$$\boldsymbol{x}^{1+1}_{n+1} = \boldsymbol{x}^1_{n+1} + \Delta\boldsymbol{x}^1_{n+1} \tag{4}$$

A special "switching" procedure (Gawin and Schrefler 1996), which allows dealing with fully and partially saturated media present at the same time in the different parts of the analyzed domain, is applied. Based on the presented discretization, the HMTRA-DEF research computer code has been

TABLE 1
Main Material Parameters of the Wall

Material property	Units	Interior plaster and exterior stucco	Cellular concrete
Dry state apparent density, ρ_o	kg/m^3 (lb/ft^3)	1860 (116.25)	463 (28.9)
Porosity, Φ	—	0.16	0.78
Thermal conductivity of dry material, $\lambda_{\mathbf{dry}}$	W/m·K (Btu·in/h·ft$^{2.}$°F)	0.9 (6.24)	0.165 (1.14)
Specific heat of dry material, $\mathbf{C_{dry}}$	J/(kg·K) (Btu/lb·°F)	940 (224.7)	850 (203.1)
Intrinsic permeability, $\mathbf{K_o}$	m^2 (ft^2)	$2.0\cdot10^{-18}$ ($2.1\cdot10^{-17}$)	$2.5\cdot10^{-17}$ ($2.7\cdot10^{-16}$)
Young's modulus, **E**	GPa (kip/in^2)	15 (2175.5)	1.5 (217.5)
Poisson's ratio, ν	—	0.15	0.25

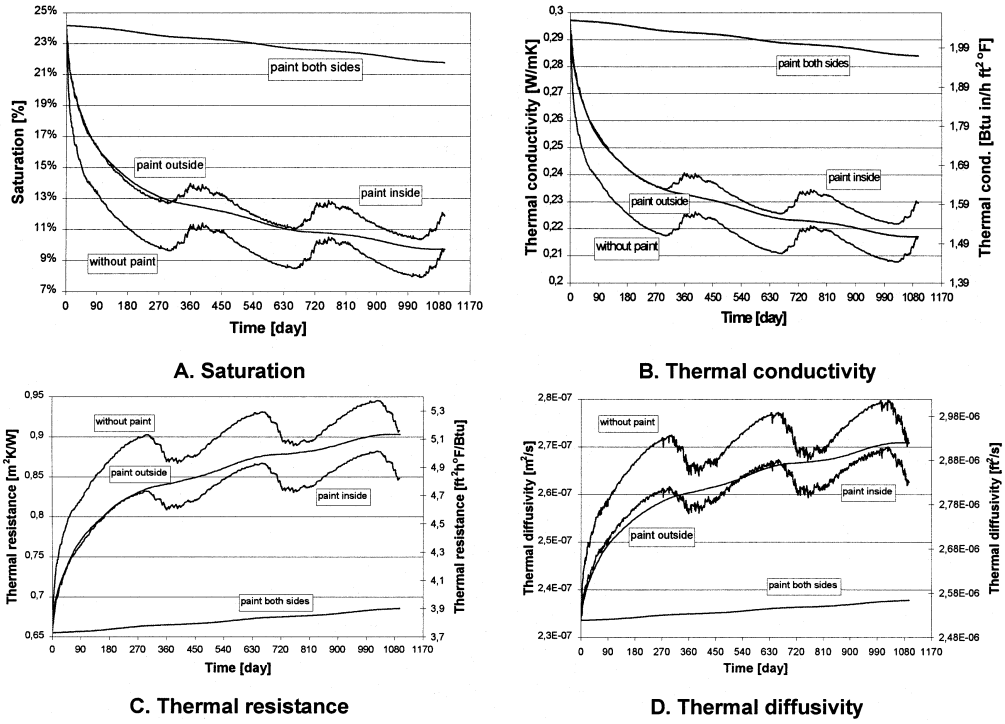

Figure 1 *Time history of the space-averaged parameters for the cellular concrete layer in Sacramento.*

developed for the solution of the nonlinear and nonsymmetrical system of equations governing heat and mass transfer in deforming porous media. It takes into account convective and/or radiative boundary conditions using hourly climatic data [e.g., in the form of test reference year (TRY) or typical meteorological year (TMY)]. The code has already been successfully applied for the solution of several problems concerning hygrothermal phenomena in building materials and soils, (e.g., Gawin et al. 1995, 1996; Gawin and Schrefler 1996).

COMPUTER SIMULATION OF HYGROTHERMAL BEHAVIOR OF A CELLULAR CONCRETE WALL

The hygrothermal behavior of a cellular concrete wall during the first three years of building use has been simulated by means of the computer model described in the previous section. The 19.8 cm (7 13/16 in.) cellular concrete wall is covered on the exterior surface with a 0.16 cm (1/16 in.) layer of stucco and on the interior surface with 0.32 cm (1/8 in.) of plaster. The main material parameters assumed in the computations are listed in Table 1.

Four different cases of finish layers on the wall surfaces are analyzed:

- both wall surfaces without vapor retarder paint;
- interior wall surface with vapor retarder paint, exterior surface without paint;
- exterior wall surface with vapor retarder paint, interior surface without paint;
- both wall surfaces covered with vapor retarder paint.

For all these cases, a vapor-retarder paint layer thickness of 70 μm and water vapor permeance of 26 ng/(s·m^2·Pa) (0.45 perm) (ASHRAE 1997) have been assumed.

At the beginning of the simulation, on January 1, the wall was assumed to be in thermodynamic equilibrium with the air, with a temperature of T = 294.15 K (70ºF) and a relative humidity φ = 95% RH. The last value was assumed to take into account water present in the pores of the materials after the construction of the wall.

On the interior surface of the wall, convective-type boundary conditions were assumed, with air temperature T_i = 294.15 K (70ºF), relative humidity φ_I = 55% RH, heat surface exchange coefficient α_i = 8.0 W/m^2·K (1.41 Btu/h·ft^2·ºF), and mass surface exchange coefficient (related to vapor density) β_i = 0.008 m/s (0.026 ft/s). On the exterior surface, convective boundary conditions were assumed as well, with α_e = 23.0 W/m^2·K (4.05 Btu/h·ft^2·ºF), β_i = 0.023 m/s (0.075 ft/s), and temperature and relative humidity of the exterior air changing over time according to TMY 2 climatic data. Simulations were done for two locations in the United States—Sacramento, California, and Miami, Florida—for a period of three consecutive years. In order to evaluate the maximal possible changes of the moisture content of the wall, and thus its thermal properties, it was assumed that the wall was not exposed to direct contact with water from falling rain. The latter condition could be important for the walls without an exterior paint layer, as it could increase their average moisture content, slowing down their average drying rate.

Figure 1 presents the resulting changes in space-averaged values of degree of saturation of pores with moisture (volume

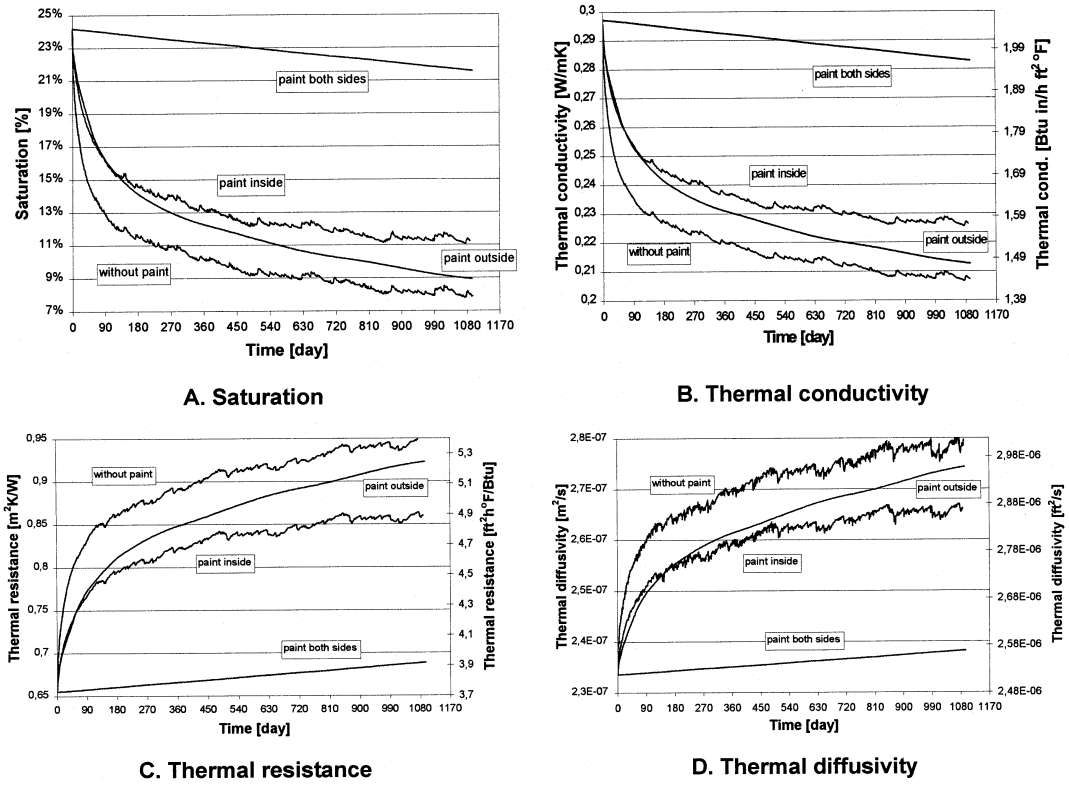

Figure 2 *Time history of the space-averaged parameters for the cellular concrete layer in Miami.*

of liquid water/volume of pores), S; thermal conductivity, λ; thermal resistance, R_T; and thermal diffusivity, a_q, for the cellular concrete layer for Sacramento climatic conditions. Corresponding results for Miami are shown in Figure 2. As could be expected, distinct differences can be observed among solutions for the various wall surface finish cases analyzed. Even the fastest drying wall, the one without any paint on the surfaces, still contains large amounts of water after three years. On average, it has a saturation of about 8% for Miami (Figure 2a) and 10% for Sacramento (Figure 1a). The three years of drying caused a decrease of about 30% in thermal conductivity (Figures 1b and 2b), an increase of about 40% in thermal resistance (Figures 1c and 2c), and an increase of about 20% in thermal diffusivity (Figures 1d and 2d). Hence, one can expect considerable differences in the energy performance of the walls, reflected in whole-building energy consumption. It is worthwhile to note the different behavior of the same walls in various climatic conditions. In Sacramento, during the period from November to January, vapor condenses inside the pores of the walls, increasing their average moisture content. In Miami, there is no such vapor condensation period, even if the drying process rate is slightly slower there for all the analyzed cases. The average moisture content in Miami after three years (at the beginning of January) is about 2% smaller than in Sacramento. All thermal properties of the analyzed cellular concrete wall change over time according to the moisture distribution history.

Using the space-averaged results of computations presented in Figures 1 and 2, the corresponding time-averaged and space-averaged values of moisture content, thermal conductivity, specific heat, and material apparent density were calculated for each month of the analyzed period. These averaged material properties were used in the building energy performance simulations presented in the next section.

RESULTS OF THE DOE 2.1E COMPUTATIONS OF WHOLE BUILDING ENERGY PERFORMANCE

The energy performance of a standard residential single-story ranch-style house was analyzed. It has been the subject of previous energy efficiency modeling studies (Hasting 1977; Huang et al. 1987; Christian 1991). A schematic of the house is shown in Figure 3. The house has ~143 m^2 (~1540 ft^2) of living area, 123.4 m^2 (1328 ft^2) of exterior (or elevation) wall area, eight windows, and two doors (one door is a glass slider, whose impact is included with the windows). The elevation wall area includes 106.5 m^2 (1146 ft^2) of opaque (or overall) wall area, 14.3 m^2 (154 ft^2) of window area, and 2.6 m^2 (28 ft^2) of door area. The following building design characteristics and operating conditions were used during computer modeling:

- Interior walls (made of 2 × 4 wood studs): 17.4 kg/m^2 (3.57 lb/ft^2) of floor area, specific heat of 0.26 Btu/lb · °F
- Furniture: 16.1 kg/m^2 (3.30 lb/ft^2) of floor area, spe-

cific heat of 1.26 kJ/(kg·K) (0.30 Btu/lb·ºF), thickness of 5.1 cm (2 in.) (total equivalent floor area)

- Thermostat setpoint: 21ºC (70ºF) for heating and 25.5ºC (78ºF) for cooling
- Window type: double-pane clear glass, with transmittance of 0.88 and reflectance of 0.08
- Roof insulation with thermal resistance of 5.28 m^2 K/W (R-30 $ft^2 \cdot h \cdot ºF$/Btu)

For calculation of infiltration, the Sherman-Grimsrud Infiltration Method option in the DOE 2.1E whole building simulation model (Sherman and Grimsrud 1980) was used. An average total leakage area of 0.0005, expressed as a fraction of the floor area, was assumed.

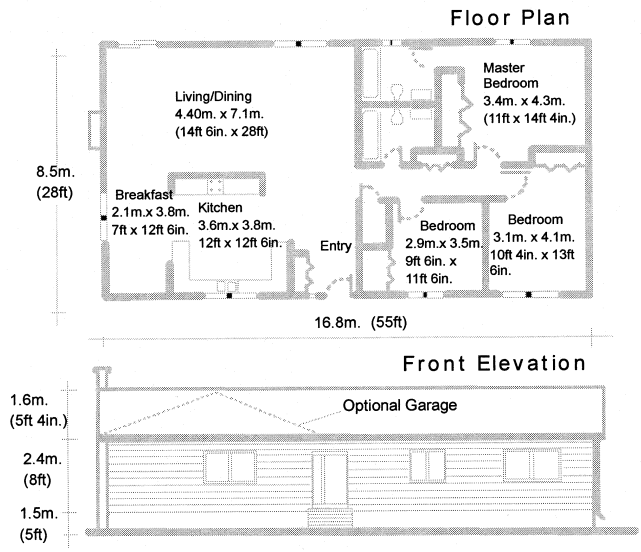

Figure 3 *Schematic of one-story ranch house used in simulations.*

Simulations were done for Sacramento and Miami, using climatic data for the TMY. Space- and time-averaged material parameters of a cellular concrete wall, different for each month of the analyzed three-year period, were used in computations to take into account changes in moisture distribution over time. Calculations were done separately for each month for four cases of the wall finish layers described in the previous section. Additionally, two limiting cases with constant thermal properties, corresponding to the initial moisture content (95% RH) and the air-dry state, were compared.

Results of the DOE 2.1E calculations concerning total energy consumption during the first 12 months are presented in Figure 4a for Miami and in Figure 5a for Sacramento. (For the next two years, their energy use was similar.) Results concerning electrical energy are shown in Figures 4b and 5b and results for natural gas energy in Figures 4c and 5c. The graphs show a very different energy-use structure for the two building locations analyzed because of climate differences. In Sacramento, the gas energy necessary for heating the building in winter dominates. In Miami, the electrical energy used for cooling dominates. In Sacramento, different levels of moisture content (resulting from different finishes on the wall) may cause an increase of up to ~18.5% in monthly energy consumption in December and January (compared with the building with dry walls). In Miami, this difference, most visible in July and August, does not exceed 7%. In Sacramento, the increase in the average wall moisture content decreases electrical energy consumption in the summer by up to ~18% and increases the gas energy for heating in the winter by up to ~19%. In Miami, we observed the opposite behavior: an increase in energy consumption of up to ~7% for cooling and a decrease of up to ~30% for winter heating in more moist walls.

TABLE 2
Comparison of Building Energy Consumption for the Wall Finish Cases Analyzed and the Dried Wall Case for Miami

Year of building use	Moist wall	Wall without paint	Wall with outside paint	Wall with inside paint	Wall with paint on both sides
Total energy					
1	103.8%	101.2%	101.4%	101.6%	103.7%
2	103.8%	100.9%	101.3%	101.3%	103.5%
3	103.8%	100.8%	100.9%	101.3%	103.3%
Electrical energy					
1	105.2%	102.0%	102.4%	102.6%	105.1%
2	105.2%	101.6%	102.0%	102.1%	104.9%
3	105.2%	101.4%	101.6%	102.1%	104.6%
Natural gas energy					
1	77.6%	85.3%	82.8%	82.8%	77.6%
2	77.6%	87.9%	87.1%	86.2%	78.4%
3	77.6%	88.8%	87.9%	86.2%	79.3%

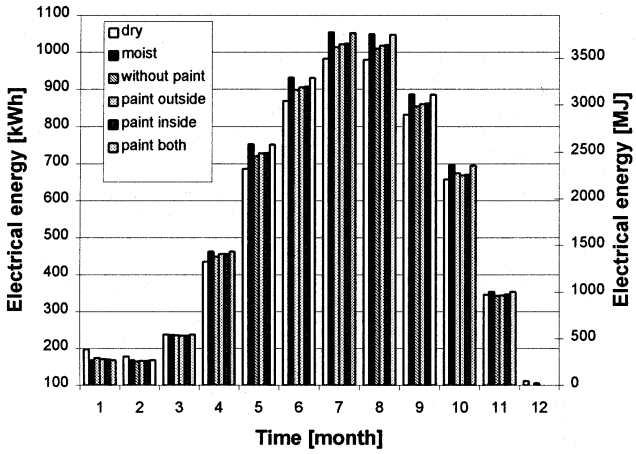

A. Total energy

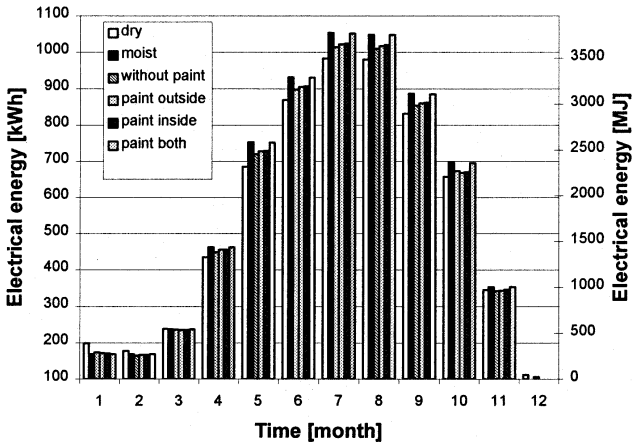

B. Electrical energy

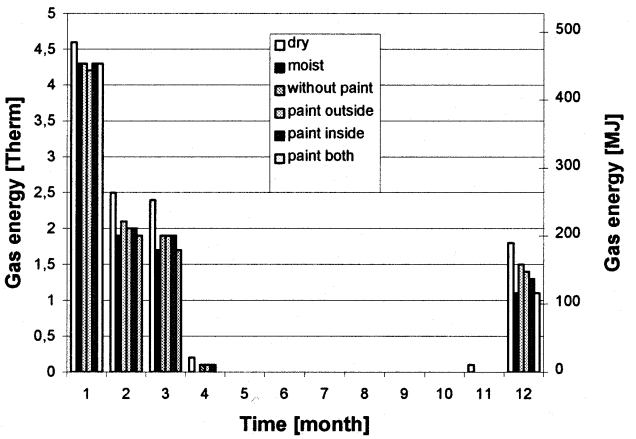

C. Natural gas energy

Figure 4 *Comparison of the energy consumption results during the first year of building use for the wall finish cases analyzed in Miami.*

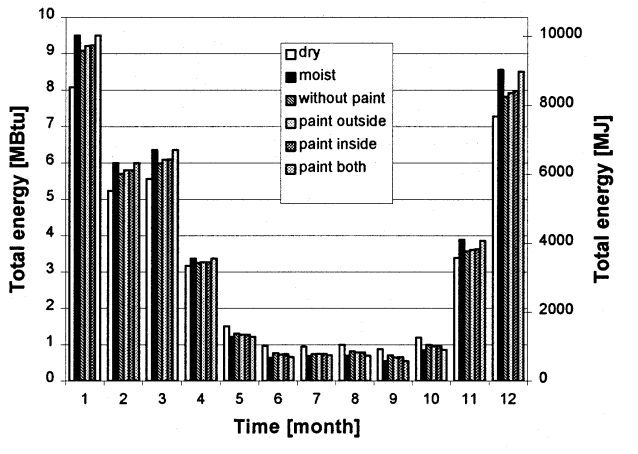

A. Total energy

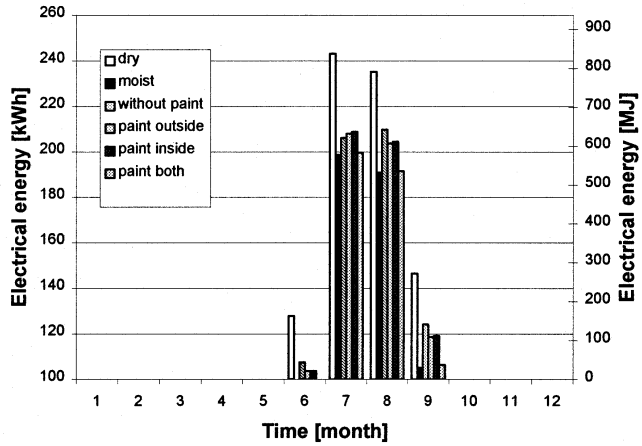

B. Electrical energy

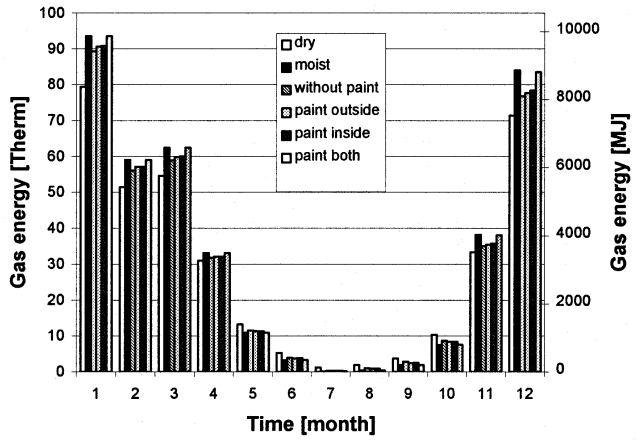

C. Natural gas energy

Figure 5 *Comparison of the energy consumption results during the first year of building use for the wall finish cases analyzed in Sacramento.*

TABLE 3
Comparison of Building Energy Consumption for the Wall Finish Cases Analyzed and the Dried Wall Case for Sacramento

Year of building use	Moist wall	Wall without paint	Wall with outside paint	Wall with inside paint	Wall with paint on both sides
Total energy					
1	107.9%	103.9%	104.6%	105.0%	107.8%
2	107.9%	102.3%	102.6%	103.3%	107.5%
3	107.9%	102.1%	102.0%	103.1%	107.1%
Electrical energy					
1	81.1%	88.0%	86.2%	86.5%	81.5%
2	81.1%	90.0%	88.0%	88.0%	81.7%
3	81.1%	90.6%	89.0%	88.5%	82.2%
Natural gas energy					
1	110.5%	105.4%	106.5%	106.9%	110.4%
2	110.5%	103.5%	104.0%	104.9%	110.0%
3	110.5%	103.2%	103.3%	104.6%	109.6%

To better analyze the effect of the wall finish layers on the whole-building energy performance during the first three years of building use, we compared the yearly consumption of total energy, electrical energy, and natural gas energy for Miami (Table 2) and Sacramento (Table 3) with the results obtained for the building with dry walls. During year 1, energy consumption for the Miami building with paint on both surfaces of the cellular concrete walls was ~3.7% for total energy consumption, ~5.1% higher for electrical energy use, and ~22.4% lower for gas energy use (comparisons are made against the same building containing dry walls). During the next two years, these differences decreased slightly. The building in Sacramento with painted cellular concrete walls had energy use that was ~7.8% higher for total energy, ~19.5% lower for electrical energy, and ~10.4% higher for gas energy.

The DOE 2.1E model does not take into account the latent heat associated with moisture evaporation and condensation. This effect could be of importance during the first period of building use, when the drying rate of the cellular concrete walls may be considerable (Figure 1a and 2a). Proper evaluation of the effect of the latent heat associated with these phenomena on the whole-building energy performance would require a whole-building hygrothermal model, which is not available at the moment. The additional energy consumption caused by the latent heat due to the changes of the wall moisture content, the vapor flux, and the related latent heat flux on the interior surface of the wall has been calculated in this paper. Boundary conditions and the results of the simulations presented in the previous section have been used for this purpose. Such an evaluation does not take into account all the additional loads for the house heating and cooling systems. This is because of the nonstationary and coupled character of heat and moisture transfer. For example, evaporation causes a decrease in wall surface temperature, which influences building heat exchange; and evaporation on exterior surface of the wall can increase the energy load for heating.

Additional monthly energy loads caused by the drying process (latent heat) on the interior surface of the walls during selected months of the three-year analysis period are presented in Figure 6. For a better analysis, Figure 7 shows the same results as a percentage of the total energy consumption for the two test locations. The negative values represent condensation of the vapor from the ambient air on the interior surface of the wall. For an estimate of the real increase in whole-building energy consumption related to these additional loads, the efficiency of the heating system (assumed to be 77% in the DOE simulations) or the coefficient of performance (COP) of the cooling system (a seasonal average value of ~2.5–3) should be taken into account (with the value dependent on the month analyzed). It should be noted that the relatively high contribution of latent heat to the total building energy consumption for the first three months in Miami (Figure 2a) was caused mainly by the small energy demand during this period. Nevertheless, analysis of Figure 7 shows that in Miami, evaporation of moisture from the walls can increase the total monthly energy consumption by up to ~2% in a cooling period and ~5% in a heating period. This analysis holds true for almost the whole period analyzed (three years). By contrast, during the first three months after building construction the heating energy required can double. The same statistics for Sacramento show that total energy consumption can increase up to ~10% in a cooling period and ~4% in a heating period.

CONCLUSIONS

During the first months after construction of a building, the moisture content of a cellular concrete wall decreases significantly. The decrease depends on the type of wall surface finish layers (and the related vapor-retarding properties) and

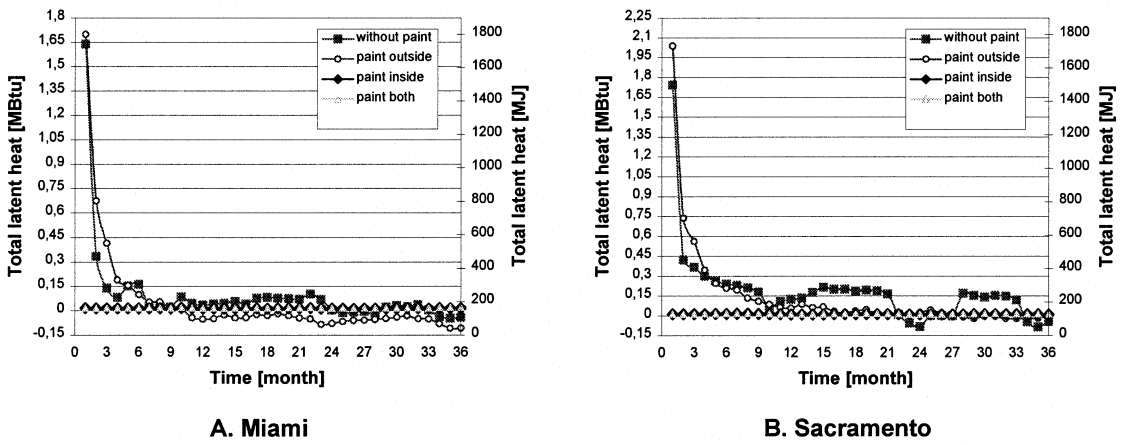

Figure 6 *Total latent heat on the interior surface of the walls due to changes of their moisture content in Miami and Sacramento.*

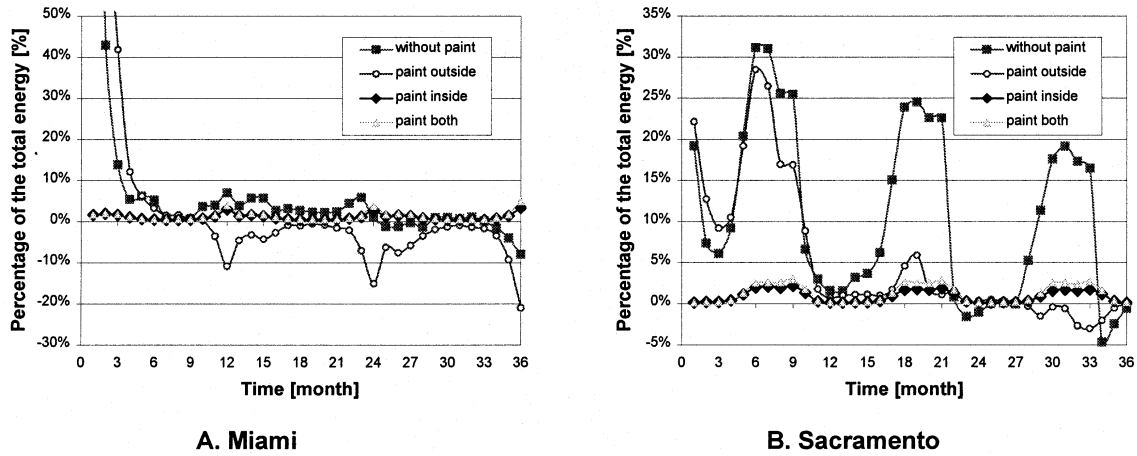

Figure 7 *Total latent heat on the interior surface of the walls as a result of changes in their moisture content as a percentage of the total energy consumption for the analyzed residential buildings in Miami and Sacramento.*

climatic conditions. This drying process can cause considerable changes in the thermal properties of cellular concrete walls; for example, it can increase their thermal resistance more than 45% compared with the initial, moist state of the walls. These changes have a notable effect on the total energy consumption in both heating and cooling periods. In the residential building analyzed, total energy consumption decreased by up to ~3.5% in Miami and ~7% in Sacramento. The process of drying the walls caused an additional increase in energy consumption that was estimated to be as much as ~2% in Miami and ~4% in Sacramento.

ACKNOWLEDGMENTS

This research was supported in part by an appointment to the Oak Ridge National Laboratory Postdoctoral Research Associates Program, administrated jointly by the Oak Ridge Institute for Science and Education and Oak Ridge National Laboratory. The first author research was also supported in part by the Polish State Committee for Scientific Research, grant No. 7 T07E 018 19.

REFERENCES

ASHRAE. 1997. *1997 ASHRAE Handbook—Fundamentals*, SI edition. Atlanta: American Society of Heating, Refrigerating and Air-Conditioning Engineers.

Burch, D. M., W. C. Thomas, L. R. Mathena, B. A. Licitra, and D. B. Ward. 1990. Transcient moisture and heat transfer in multilayer non-isothermal walls: Comparison of predicted and measured results. *Thermal Performance of the Exterior Envelopes of Buildings IV,* pp. 513–531. Atlanta: American Society of Heating, Refrigerating and Air-Conditioning Engineers, Inc.

Burch, D. M., G. A.Tsongas, and G. N. Walton. 1996. Mathematical analysis of practices to control moisture in the roof cavities of manufactured houses. NISTIR 5880. Washington, D.C.: National Institute of Standards and Technology, September.

Christian, J. E. 1991. Thermal mass credits relating to building energy standards. *ASHRAE Transactions* 97 (2).

FSEC. 1992. FSEC 3.0: Florida software for environmental computation. FSEC-GP-47-92. Cocoa, Fla.: Florida Solar Energy Center.

Gawin, D., P. Baggio, and B. A. Schrefler. 1995. Coupled heat, water and gas flow in deformable porous media. *International Journal of Numerical Methods in Fluids*, 20:969–987

Gawin, D., P. Baggio, and B. A. Schrefler. 1996. Modelling heat and moisture transfer in deformable porous building materials. *Archives of civil engineering* 42:325–349

Gawin, D., and B. A. Schrefler. 1996. Thermo-hydro-mechanical analysis of partially saturated porous materials. *Engineering computations* 13 (7): 113–143

Gawin, D., J. Kosny, and A. Desjarlais. 2000. The effect of moisture content on accuracy of the steady state thermal conductivity tests for light-weight concretes. *Proceedings of ACEEE Summer Study on Energy Efficient Economy, Monterey, Calif., August*.

Hasting, S. R. 1977. Three proposed typical house designs for energy conservation research. NBSIR 77-1309. Gaithersburg, Md.: National Bureau of Standards.

Huang, Y. J., J. Rirschard, S. Bull, I. Byrne, D. Turiel, C. Wilson, H. Sui, and D. Folley. 1987. Methodology and assumptions for evaluating heating and cooling energy requirements in new single-family residential buildings: Technical support document for the PEAR Microcomputer Program. LBL-19128. Berkeley, Calif.: Lawrence Berkeley National Laboratory, University of California.

Karagiozis, A., M. Salonvaara, and K. Kumaran. 1994. LATENITE hygrothermal material property database. IEA Annex 24 Report TI-CA-94/04. Trondheim, Norway: International Energy Agency.

Kohonen, R. 1984. A method to analyze the transient hygrothermal behaviour of building materials and components. Ph. D. dissertation, VTT, Espoo, Finland.

Kuenzel, H. M. 1994. Verfahren zur ein- and zweidimensionalen Berechnung des gekoppelten Waerme- and Feuchtetransports in Bauteilen mit einfachen Kennwerten. Ph.D. dissertation, University of Stuttgart.

Pedersen, C. (name changed to C. Rode). 1990. Combined heat and moisture transfer in building constructions. Ph. D. dissertation, Technical University of Denmark, Thermal Insulation Laboratory.

Rode, C., and G. E. Courville. 1991. A computer analysis of the annual thermal performance of roof system with slightly wet fibrous glass insulation under transient conditions. *Journal of Thermal Insulation*, 15:110–136.

Salonvaara, M., and A. Karagiozis. 1994. Moisture transport in building envelopes using an approximate factorization solution method. CFD Society of Canada, Toronto June 1–3.

Sherman, M. H., and D. T. Grimsrud. 1980. Measurement of infiltration using fan pressurization and weather data. LBL-10852. Berkeley, Calif.: Lawrence Berkeley Laboratory, University of California, October.

Zienkiewicz, O. C., and R. L. Taylor. 1989. *The finite element method*, Vol. 1, 4th ed. London: McGraw Hill.

Zienkiewicz, O. C., and R. L. Taylor. 1991. *The finite element method*, Vol. 2, 4th ed. London: McGraw Hill.